ACADEMIC PRESS

Available online at www.sciencedirect.com
SCIENCE DIRECT®

Journal of Catalysis 213 (2003) 191–203

JOURNAL OF CATALYSIS

www.elsevier.com/locate/jcat

Dry reforming of methane over catalysts derived from nickel-containing Mg–Al layered double hydroxides

Andrey I. Tsyganok,[a,*] Tatsuo Tsunoda,[a] Satoshi Hamakawa,[a] Kunio Suzuki,[a] Katsuomi Takehira,[b] and Takashi Hayakawa [a]

[a] *National Institute of Advanced Industrial Science and Technology (AIST), Institute for Materials and Chemical Process, Tsukuba Central 5, Higashi 1-1-1, Tsukuba 305-8565, Japan*

[b] *Department of Applied Chemistry, Faculty of Engineering, Hiroshima University, Kagamiyama 1-4-1, Higashi-Hiroshima 739-8527, Japan*

Received 31 May 2002; revised 6 September 2002; accepted 16 September 2002

Abstract

We present the synthesis and structural characterization of new nickel-containing Mg–Al layered double hydroxides (LDH), which adopt a structure in which nickel, chelated with ethylenediaminetetraacetate to a divalent anion $[Ni(EDTA)]^{2-}$, is nested between brucite-like layers of LDH. The corresponding LDH-derived Ni–Mg–Al mixed oxides demonstrated high and stable catalytic function toward the reaction of methane reforming with carbon dioxide into synthesis gas at 800 °C. It is shown that the state of the supported nickel and the coke deposition process were significantly influenced by the method of catalyst preparation.

Keywords: Methane; Dry reforming; Synthesis gas; Nickel catalysts; Layered double hydroxides; Intercalation

1. Introduction

Supported nickel catalysts are used in industrially important reactions for producing hydrogen and synthesis gas from hydrocarbon feedstock [1–7]. Manufacturing such catalysts at a lower cost gives them an advantage in relation to supported noble metals, although the problem of coke formation leading to deactivation of nickel catalysts is often pointed out [8–12].

Synthetic Mg–Al layered double hydroxide materials similar to the naturally occurring hydrotalcite ($[Mg_6Al_2(OH)_{16}]CO_3 \cdot 4H_2O$) have found many applications due to their unique physicochemical properties [13–16]. By additional modification, such materials can be converted to catalyst precursors or directly to catalysts of many useful reactions.

The conventional way to prepare nickel-containing Mg–Al mixed oxide catalysts via LDH precursor includes co-precipitation of Ni^{2+}, Mg^{2+}, and Al^{3+} with a carbonate counterion at basic pH. Due to their nearly equal cation size, nickel(II) isomorphously replaces magnesium(II) within brucite-like layers of LDH, thus giving a structure very similar to that of hydrotalcite (Fig. 1A). Such a technique was used to preparing catalysts for partial oxidation of methane [17,18] and propane [19,20] and dry reforming of methane, DRM [21].

It was recently reported [22] that nickel could be introduced into Mg–Al LDH by an alternative technique. It involved co-precipitation of Mg^{2+} and Al^{3+} with a presynthesized complex of Ni(II) with ethylenediaminetetraacetate (i.e., $[Ni(EDTA)]^{2-}$, to be denoted hereafter as NiY^{2-}) giving rise to a new LDH phase (denoted *cp*-MgAl-NiY in Table 1), where chelated nickel species reside within the interlayer space (Fig. 1B). The formation of such a structure was confirmed with results of powder X-ray diffraction (XRD), diffuse reflectance Fourier-transform infrared spectroscopy (DRIFT), thermogravimetry and differential thermal analysis (TG-DTA), and elemental analysis studies. Calcination of LDH in air yielded a Ni–Mg–Al mixed oxide that upon preliminary reduction with hydrogen afforded high, durable, and reusable catalytic function toward dry reforming of methane (i.e., reforming of methane with carbon dioxide into synthesis gas [23]),

$$CH_4 + CO_2 = 2H_2 + 2CO. \quad (1)$$

* Corresponding author.
E-mail addresses: andrey-tsyganok@aist.go.jp (A.I. Tsyganok), t.hayakawa@aist.go.jp (T. Hayakawa).

0021-9517/02/$ – see front matter
PII: S0021-9517(02)00047-7

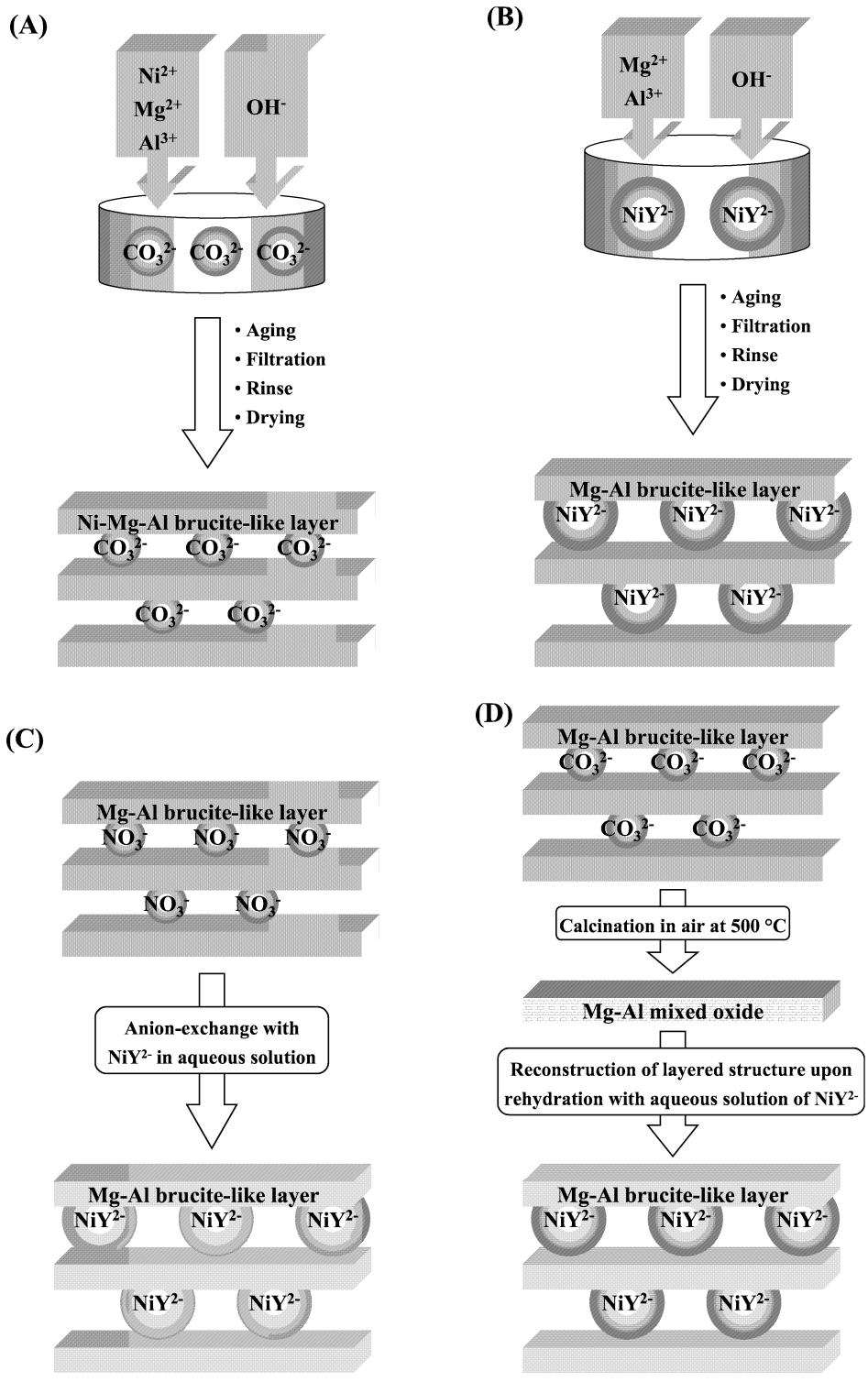

Fig. 1. Synthetic pathways for introduction of nickel into Mg–Al layered double hydroxides ($[Ni(EDTA)]^{2-}$ chelate is denoted NiY^{2-}).

The anion-exchange capacity of Mg–Al LDHs is well known and widely used in catalysis as a tool by means of which component(s) offering a target activity and/or selectivity can be introduced [24–26]. It will be shown that such a technique can readily be applied to synthesizing NiY^{2-}-containing Mg–Al LDH, *ae*-MgAl–NiY (Fig. 1C), which gives in turn a suitable mixed oxide catalyst of DRM. Furthermore, the ability of calcined Mg–Al mixed oxide to reconstruct the hydrotalcite-like layered structure upon rehydration with an aqueous solution is also well known [27–29]. In this paper, we shall demonstrate that by such a technique the NiY^{2-}-bearing Mg–Al LDH, i.e., *rc*-MgAl–

Table 1
Ni-containing Mg–Al layered double hydroxides and the corresponding Ni–Mg–Al mixed oxide catalysts

Method of LDH synthesis	Legend for synthesized LDH	Formula of mixed oxide (from ICP-AES data)	Specific surface area of Ni–Mg–Al mixed oxide (m^2g^{-1})	Legend for Ni–Mg–Al mixed oxide catalyst
1. Co-precipitation of Mg^{2+} and Al^{3+} with pre-synthesized $[Ni(edta)]^{2-}$ chelate	*cp*-MgAl–NiY	$NiMg_7Al_2O_{11}$	115.7	*cp*-Ni/$MgAlO_x$
2. Anion-exchange reaction of NO_3^- of MgAl–NO_3 LDH with $[Ni(EDTA)]^{2-}$ chelate in an aqueous solution	*ae*-MgAl–NiY	$NiMg_{11}Al_{3.3}O_{17}$	102.3	*ae*-Ni/$MgAlO_x$
3. Reconstruction of LDH structure for Mg–Al mixed oxide in an aqueous solution of $[Ni(EDTA)]^{2-}$	*rc*-MgAl–NiY	$NiMg_{11}Al_3O_{16.5}$	102.4	*rc*-Ni/$MgAlO_x$
4. Co-precipitation of Ni^{2+}, Mg^{2+}, and Al^{3+} with CO_3^{2-} (traditional technique)	*tr*-NiMgAl–CO_3	$NiMg_5Al_2O_9$	139.0	*tr*-Ni/$MgAlO_x$

NiY, can be synthesized (Fig. 1D). The results of catalytic activity tests of Ni–Mg–Al mixed oxides derived from such LDHs will be presented and discussed. Activity of LDH-derived catalysts will be compared with that of catalysts synthesized by other methods.

Particular attention in this work will be focused on (i) deposition of coke onto nickel catalyst surface, (ii) state and spatial distribution of supported nickel after reaction, and (iii) thermal stability of nickel catalysts supported on Mg–Al mixed oxide.

2. Experimental

2.1. Reagents and materials

All the reagents used in this study were purchased from Wako Pure Chemical Industries, Ltd. Chemicals had 98–99% purity and were used without additional purification. Distilled and deionized water was used throughout the work. Methane and carbon dioxide were from Tokyo Gas Chemical Co. and Showa Tansan Co. Pipeline nitrogen gas was used to dilute the feeding gas mixture. All the gases were of purity higher than 99.99%.

The reference materials, employed in this work, included (i) Mg–Al mixed oxide ($MgAlO_x$; particle size 212–425 μm) prepared from $[Mg_6Al_2(OH)_{16}]CO_3$ synthetic hydrotalcite (MgAl–CO_3) by calcination in air at 500 °C for 16 h, (ii) $[Mg_3Al(OH)_8]NO_3$ double hydroxide (MgAl–NO_3), (iii) colorless solid of Mg(II) and Al(III) nitrates (1 : 2 by mol) obtained from an aqueous solution of the salts by evaporation of water, and (iv) physical mixture of MgO (0.1 μm; 99.9%) and α-Al_2O_3 (1 μm; 99%) of molar ratio 1 : 1, favorable for the formation of $MgAl_2O_4$ spinel. To prepare the mixture, the powders were placed in a screw-cap vial of capacity 20 cm^3 that was horizontally rotated at 100 rpm at room temperature for 24 h.

2.2. Synthesis of LDHs

The detailed procedure of synthesizing *cp*-MgAl–NiY LDH was reported elsewhere [23].

To prepare the *ae*-MgAl–NiY sample, the MgAl–NO_3 powder (4.98 g; ca. 14.9 mmol) was placed in a conical flask filled with a 200 cm^3 aqueous solution of presynthesized NiY^{2-} chelate (67 mmol). Prior to addition of the solid, the solution pH was adjusted to 10.5 by adding a 1.0 M solution of NaOH. The resultant suspension was vigorously stirred with a teflon-coated magnet bar at 25 °C for 24 h. To minimize contamination of LDH with carbonate from CO_2 of air, the flask was kept tightly closed. The synthesized pale-blue solid was then separated by filtration, rinsed with the distilled and deionized water until the filtrate was free from NiY^{2-} chelate, dried in air at 80 °C for 16 h, and kept in a desiccator under vacuum at room temperature.

The first step of *rc*-MgAl–NiY synthesis involved preparation of an aqueous solution of NiY^{2-} chelate (49 mmol in 200 cm^3 of water) according to the technique already reported [23]. The solution pH was adjusted to 10.5 by adding an aqueous 1.0 M sodium hydroxide. Then the fine powder of Mg–Al mixed oxide (1.72 g; ca. 5.0 mmol) prepared from calcined MgAl–CO_3 was introduced. The suspension was left under intensive stirring at 25 °C for 24 h. During the experiment, a conical flask was kept well closed in order to minimize contamination of LDH with CO_2 from air. Afterwards, the synthesized *rc*-MgAl–NiY was treated the same way as *ae*-MgAl–NiY.

Traditional synthesis of Ni-containing Mg–Al layered hydroxide included dropwise addition of an aqueous solution (100 cm^3) containing Ni(II), Mg(II), and Al(III) nitrates (5, 25, and 10 mmol) to a solution of sodium carbonate (30 mmol in 200 cm^3 water) kept at 63 °C. The suspension pH was kept at 10.0 by addition of 1.0 M NaOH aqueous solution. The slurry was intensively stirred with a teflon-coated bar magnet at 63 °C for all the time of solution addition. After the solution of metal cations was completely added, the suspension was stirred at 63 °C for an hour. Then followed the step of precipitate aging at the same temperature

for 18 h without stirring. Thus-synthesized *tr*-NiMgAl–CO_3 LDH having a light-green color was separated by filtration, rinsed with 2 l of distilled and deionized water, dried in air at 80 °C for 16 h, and kept under vacuum in a desiccator.

Calcination of all the synthesized Ni-containing Mg–Al LDHs at 500 °C for 16 h yielded Ni–Mg–Al mixed oxides (Table 1) that were stored in a desiccator and thereafter used as catalysts.

2.3. Characterization techniques

X-ray diffraction patterns of powdered samples were recorded at room temperature under air using a MacScience MXP18 diffractometer with a Cu-K_α irradiation source ($\lambda = 1.54056$ Å) at voltage 40 kV and current 50 mA.

TG-DTA studies of LDHs were carried out under an inert (20 $cm^3\,min^{-1}$ of N_2) atmosphere with TGA-50 and DTA-50 analyzers (both from Shimadzu Co.) using 30 to 50 mg of sample and 10 °C min^{-1} temperature increase rate.

Specific surface area of Ni–Mg–Al mixed oxides was measured by adsorption of N_2 at liquid nitrogen temperature using Shimadzu Micromeritics FlowSorb II 2300 analyzer with an N_2–He (33 : 67 by volume) gas mixture. A powder sample (30 to 35 mg) was outgassed at 100 °C for 1 h and then cooled to room temperature before area measurement. After several adsorption–desorption cycles the average values of BET surface areas were calculated (Table 1).

The elemental composition of Ni–Mg–Al mixed oxides was determined using a Thermo Jarrel-Ash IRIS/AP Model inductively coupled plasma atomic emission spectrometer (ICP-AES). Every mixed oxide was first dissolved in a small volume of concentrated nitric acid and then diluted by water to a concentration level suitable for ICP-AES measurements. On the basis of ICP-AES results, the formulas of Ni–Mg–Al mixed oxides were retrieved (Table 1).

Transmission electron microscopy (TEM) was done with a JEOL JEM-2010F machine equipped with a Gatan slow-scan camera for high-resolution observation. The accelerating voltage applied was 200 kV. Specimens for TEM were prepared by standard techniques.

DRIFT spectra were recorded with a Nicolet Magna-IR 750 spectrometer equipped with a chamber for DRIFT measurements, a KBr beam splitter, a DTGS (KBr) detector, and a He–Ne laser ($\lambda = 633$ nm). A chamber with powdered sample was purged with nitrogen (40 $cm^3\,min^{-1}$) for 30 min prior to every DRIFT measurement. Data acquisition for each sample involved 200 scans taken within 4 min with resolution 4 cm^{-1} at room temperature under nitrogen flow.

2.4. Catalytic activity tests

Every Ni–Mg–Al mixed oxide was pressed into a tablet and ground up to sieve 212–425 μm fraction of particles that was used for catalytic experiments. The catalyst (150 mg) was well mixed with Wakogel silicas G (250 mg; 300–600 μm) and C-100 (250 mg; 150–425 μm). The vertically mounted quartz tube reactor (8 mm i.d.) was charged with a mixture of catalyst and silica, and gases were introduced with upstream flow direction. Activation of the Ni-catalyst involved reductive treatment with hydrogen (H_2–N_2 10 : 35 $cm^3\,min^{-1}$) at 600 °C for 15 min followed by cooling to room temperature under pure nitrogen. Then reactor was fed with a reagent gas mixture of CH_4–CO_2–N_2 (25 : 25 : 35 $cm^3\,min^{-1}$) and heated at 5.0 °C min^{-1}. When the temperature of the reactor reached 800 °C, the sampling of post-reactor gas phase was started. Analysis of reaction products was carried out by gas chromatography (GC) using Porapak Q and molecular sieve 5A packed columns. After 6 h time on stream at 800 °C admission of methane and carbon dioxide was stopped, and the reactor was cooled to room temperature under flow of nitrogen.

2.5. Evaluation of catalytically produced coke

To measure the amount of coke produced over nickel catalysts under DRM conditions, each Ni–Mg–Al mixed oxide (212–425 μm) was taken in a 300 mg amount, was loaded into the reactor without silica, and was not reductively pretreated with hydrogen. Feed gas mixture (CH_4–CO_2–N_2) was introduced upstream with the same flow rate as that of catalytic tests. The reactor was heated to 800 °C at 5.0 °C min^{-1} followed by keeping temperature at 800 °C for 6 h. When the stated time elapsed, admission of methane and carbon dioxide was stopped, and the reactor was cooled to room temperature under nitrogen flow. A comparative blank trial was performed with a nickel-free $MgAlO_x$ sample (500 mg; 212–425 μm) prepared from Mg–Al–CO_3. The black powder of a spent catalyst was removed from the reactor and kept in a 5 cm^3 screw-cap vial under air. To quantify the catalytically produced coke by the TG-DTA technique, a spent catalyst (30 to 50 mg loading) was subjected to temperature-programmed oxidation from room temperature to 1000 °C at 5.0 °C min^{-1} under a 20 $cm^3\,min^{-1}$ flow of air.

3. Results and discussion

3.1. Incorporation of nickel into layered structure of Mg–Al double hydroxides

The results of XRD measurements of Ni-containing LDHs and reference materials are shown in Fig. 2. The structure of LDH, prepared by co-precipitation of Mg(II) and Al(III) with preformed NiY^{2-} chelate, had already been characterized in detail [23]. One should here mention that incorporation of NiY^{2-} species resulted in appearance of three peaks at 2Θ 6.0°, 12.1°, and 18.4° (pattern A in Fig. 2) which were assigned to X-ray reflections from (003), (006), and (009) planes of newly synthesized LDH. The corresponding values of 14.7 Å (d), 7.8 Å (as $d/2$), and 4.8 Å (as $d/3$) were obtained, which suggested that

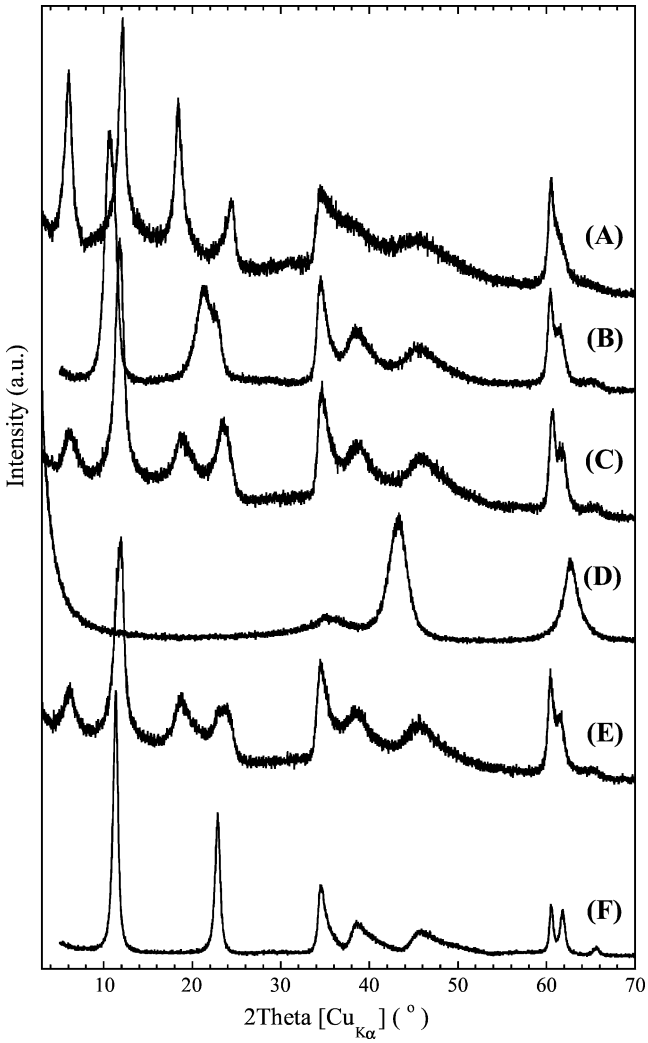

Fig. 2. X-ray powder diffraction patterns of Mg–Al double hydroxides and references: *cp*-MgAl–NiY (A), MgAl–NO_3 (B), *ae*-MgAl–NiY (C), $MgAlO_x$ (D), *rc*-MgAl–NiY (E), and *tr*-NiMgAl–CO_3 (F).

intercalation of the NiY^{2-} chelate caused an expansion in intergallery distance to 9.9 Å from 3 Å of reference MgAl–CO_3.

The anion-exchange reaction, done with MgAl–NO_3 and an aqueous solution of NiY^{2-}, resulted in formation of a phase that strikingly differed from that of the starting material (compare patterns B and C in Fig. 2). Three new reflection peaks appeared at 2Θ 6.0°, 11.8°, and 18.6°, the peak at 11.8° being the most intensive. We believe this peak represents a superposition of two contributing peaks, namely, the one at 12.1° (as reflection from the (006) plane of the *ae*-MgAl–NiY phase) and that at 11.3° which related to the reflection from the (003) plane of an impurity hydrotalcite-like carbonate phase, formed upon absorption of CO_2 from air.

Calcination of MgAl–CO_3 at 500 °C for 16 h completely destroyed the layered structure of LDH. A powder XRD pattern similar to that of periclase MgO was registered (pattern D). However, after rehydration of such a Mg–Al mixed oxide with an aqueous NiY^{2-} solution the lamellar structure was recreated, which was confirmed with XRD: a pattern (E) nearly the same as that of *ae*-MgAl–NiY was registered.

When Ni(II) was co-precipitated as a cationic species together with Mg^{2+}, Al^{3+}, and carbonate counteranion, a phase having practically the same parameters of layered structure as those of MgAl–CO_3 was formed (see pattern F in Fig. 2).

The results of TG-DTA measurements strengthened the difference in properties of Ni-containing LDHs synthesized by intercalation and by traditional techniques (Fig. 3). All the NiY^{2-}-involving lamellar solids revealed a two-step reduction in sample weight, the largest being at 380–440 °C (TG-profiles A to C in Fig. 3). The corresponding DTA-profiles (A* to C*) also resembled each other, demonstrating three viewable endothermic peaks. A temperature around 100 °C was sufficient for removing physisorbed water whereas desorption of structural water required a higher temperature (i.e., 220–230 °C). The third intensive endothermic peak, positioned at 416–420 °C, was assigned to dehydroxylation of Mg(II) and Al(III) hydroxides, collapse of a layered structure, and decomposition of entrapped NiY^{2-} species [22]. Thermal decomposition of *tr*-NiMgAl–CO_3 occurred in two steps, as is typical of Mg–Al LDHs [13]. However, the difference in sample weight reduction for step 1 (40 to 260 °C) and step 2 (300 to 700 °C) was not so pronounced, as was observed with NiY^{2-}-intercalated LDHs. Moreover, only two endothermic peaks were recorded with the DTA analyzer (profile D*), suggesting that the content of structural water dominated over that of water physisorbed in *tr*-NiMgAl–CO_3 and a noticeably lower temperature (404 °C) was required for dehydroxylation, collapse of layered structure, and desorption of CO_2 from carbonate.

To confirm incorporation of NiY^{2-} species into *ae*- and *rc*-MgAl–NiY samples, DRIFT spectroscopy was applied. The spectra recorded were very similar to that of *cp*-MgAl–NiY that had already been reported [23]. The characteristic strong absorption at 1640 cm^{-1}, related to stretching of COO^- groups coordinated to Ni(II), and absorption of lower intensity at 2800–3000 cm^{-1} due to C–H stretching of methylene groups of NiY^{2-} chelate, were registered for all the samples, indicating that nickel chelate kept its integrity upon insertion into the LDH matrix.

3.2. Nickel-catalyzed reforming of methane with carbon dioxide to synthesis gas

All the synthesized Ni-containing Mg–Al LDHs were calcined in air at 500 °C for 16 h in order to obtain Ni–Mg–Al mixed oxides to be used further for catalytic tests (Table 1). Analysis of the elemental composition of all the resultant mixed oxides, with the exception of *tr*-Ni/$MgAlO_x$, revealed Mg-to-Al ratios higher than the starting value (Mg : Al = 3 : 1). This implied that some leaching of aluminum did occur, which we attribute to the

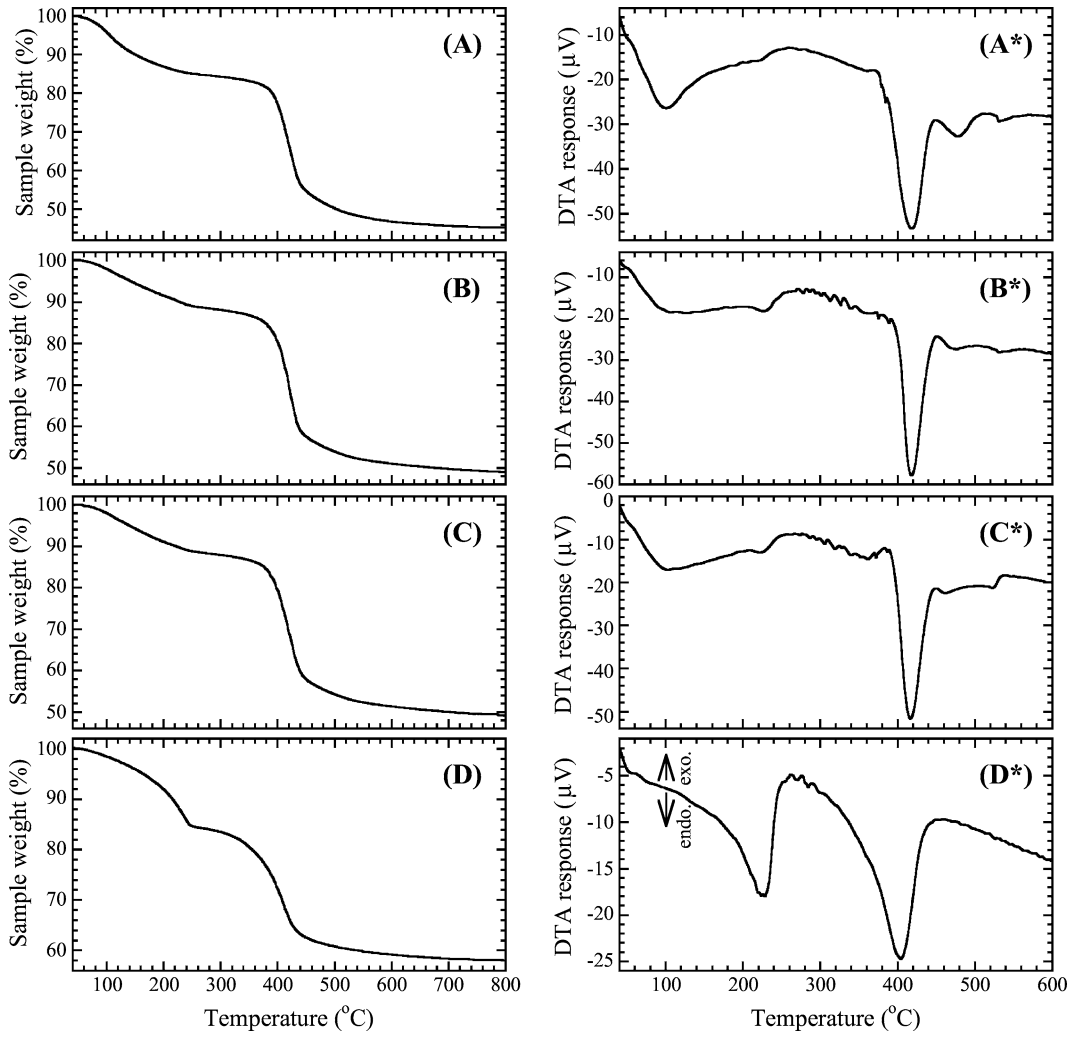

Fig. 3. TG-DTA behavior of LDH materials: *cp*-MgAl–NiY (A, A*), *ae*-MgAl–NiY (B, B*), *rc*-MgAl–NiY (C, C*), and *tr*-NiMgAl–CO_3 (D, D*).

formation of water-soluble aluminate [30] from aluminum hydroxide at moderately high basic pH,

$$Al(OH)_3 + OH^- = AlO_2^- + 2H_2O. \quad (2)$$

Catalytic activity tests involved the preliminary reductive treatment of Ni–Mg–Al mixed oxide with hydrogen, as mentioned in the Experimental Section. Then the solids were subjected to DRM at 800 °C for 6 h. In addition to LDH-derived samples, two more nickel-containing mixed oxides were tested. They were $Ni_{0.2}/Ca_{0.8}Sr_{0.2}TiO_3$ mixed oxide prepared by the sol–gel method (*sg*-Ni/CaSrTiO_Y), whose catalytic activity toward DRM was already reported [31,32], and $Ni_{0.2}/Ca_{0.8}Sr_{0.2}ZrO_3$ solid synthesized by the cellulose-template method [33,34], the latter being denoted *ctm*-Ni/CaSrZrO_Y hereafter. The both were reductively pretreated with hydrogen in the same way as LDH-derived samples and exposed to a CH_4–CO_2–N_2 reaction atmosphere for catalytic activity tests.

The results obtained for CH_4 and CO_2 conversion and selectivity to H_2 and CO are shown in Fig. 4. The first feature that can be readily drawn is that the LDH-derived nickel catalysts greatly catalyzed DRM reaction giving close to equilibrium values of CH_4 and CO_2 conversions with high selectivity to syngas components. Conversion of carbon dioxide was 2–3% higher than that of methane due to the side reaction of reversed water gas shift,

$$CO_2 + H_2 = CO + H_2O. \quad (3)$$

An other feature of catalytic behavior of LDH-derived Ni-catalysts was their sustainable working function toward DRM, as no any viewable decrease in activity and/or selectivity was observed.

Compared to LDH-derived catalysts, the catalyst prepared by the sol–gel technique revealed lower conversions of CH_4 and CO_2. Although these steadily elevated with time on stream, they did not achieve the conversion values of CH_4 and CO_2 (95 and 98%) attained with catalysts prepared from LDH precursors. For the catalyst prepared by the cellulose-template method, activity toward DRM at 800 °C was much less pronounced. Especially mentioned here should be its low selectivity to hydrogen, which implied that most of the produced H_2 was reacting with carbon dioxide to carbon

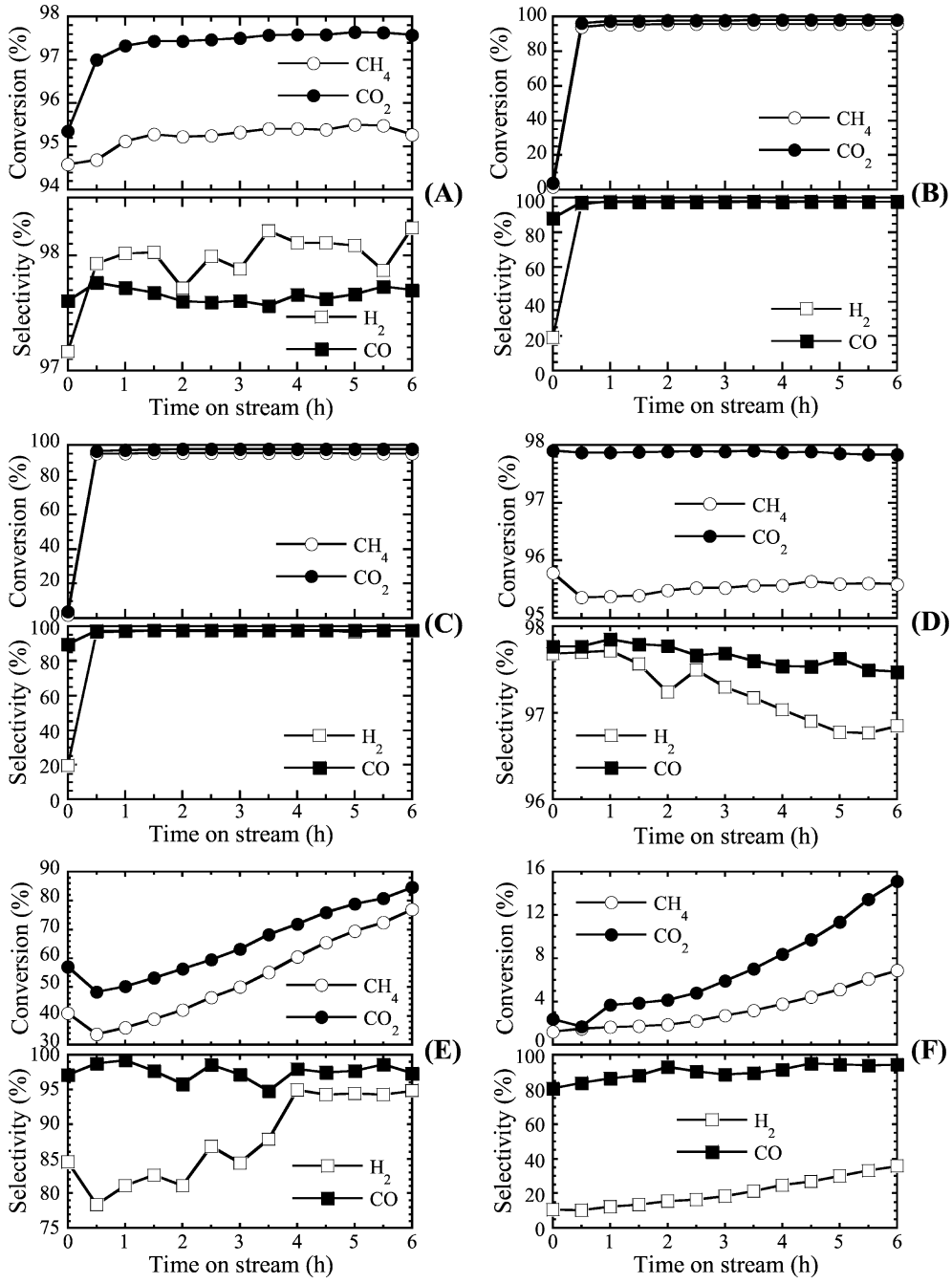

Fig. 4. Dry reforming of methane at 800 °C over prereduced nickel catalysts: *cp*-Ni/MgAlO$_x$ (A), *ae*-Ni/MgAlO$_x$ (B), *rc*-Ni/MgAlO$_x$ (C), *tr*-Ni/MgAlO$_x$ (D), *sg*-Ni/CaSrTiO$_Y$ (E), and *ctm*-Ni/CaSrZrO$_Y$ (F).

monoxide and water. Indeed, GC-analysis of the postreactor effluent gas phase using Porapak Q column revealed a considerable content of water vapor, the highest for all the tested nickel catalysts.

As can be seen in Fig. 4, high catalytic activity and selectivity to synthesis gas of reductively pretreated *ae*- and *rc*-Ni/MgAlO$_x$ samples was achieved only after 30 min time on stream. This indicated that preliminary treatment of Ni–Mg–Al mixed oxides with hydrogen at 600 °C for 15 min was not enough to completely reduce the nickel oxide phase to catalytically active metallic nickel. Also, these results strongly suggested that the supported nickel oxide would directly be reduced under the DRM reaction conditions, for example, by methane,

$$4\mathrm{NiO} + \mathrm{CH_4} = 4\mathrm{Ni^0} + \mathrm{CO_2} + 2\mathrm{H_2O}. \quad (4)$$

This would allow elimination of reductive pretreatment of catalyst as a necessary experimental step, and therefore shorten the time necessary for catalyst preparation. On the other hand, it would necessitate an induction time for the catalyst to gain high activity and selectivity.

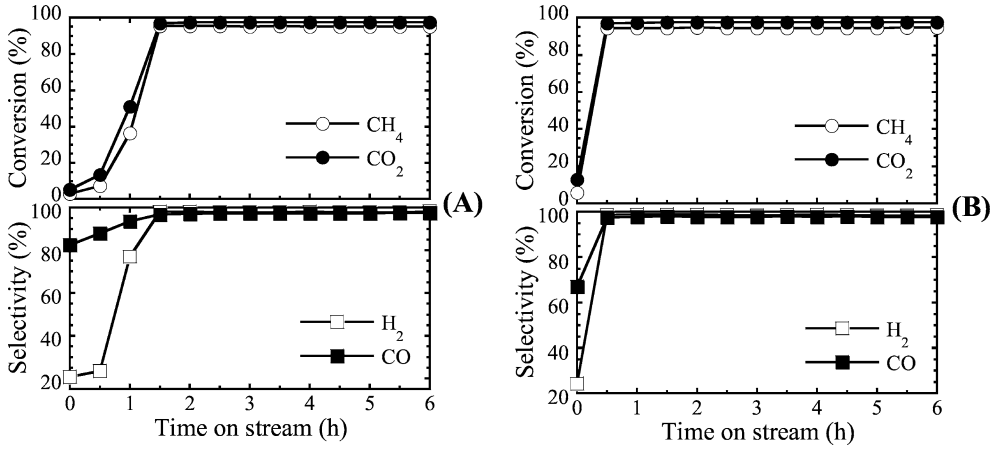

Fig. 5. Reforming of methane with carbon dioxide at 800 °C over nonreduced catalysts: *cp*-Ni/$MgAlO_x$ (A) and *tr*-Ni/$MgAlO_x$ (B).

To verify this assumption, the DRM reaction was performed over *cp*- and *tr*-Ni/$MgAlO_x$ mixed oxides which were not pretreated with hydrogen. The results obtained are shown in Fig. 5. It is seen that high and sustainable catalytic activity of both samples was approachable but required an induction time of about 1.5 h for *cp*-Ni/$MgAlO_x$ and 0.5 h for *tr*-Ni/$MgAlO_x$ catalyst. Such an experimentally found property may serve as a considerable advantage of LDH-derived nickel catalysts relative to those prepared from solid solutions of $Ni_xMg_{(1-x)}O$ and $Ni_xMg_{(1-x)}Al_2O_4$ spinels. According to the literature [35–45], the reductive pretreatment of Ni-containing solid solutions and spinels at 790–900 °C must be applied in order to initiate a catalytic function of supported nickel toward DRM reaction. Otherwise the reaction was not catalytically promoted or required a much longer induction time [37,39].

3.3. Characterization of LDH-derived nickel catalysts subjected to the DRM reaction at 800 °C

Such points of nickel-catalyzed DRM as the state of supported nickel after reaction and the formation of carbonaceous deposits that might lead to catalyst deactivation were among the special concerns of this work. To address those issues, every LDH-derived mixed oxide taken in a 300 mg amount was subjected to DRM at 800 °C for 6 h without dilution with silica and pretreatment with hydrogen. After the DRM experiment the cooled black powders of spent catalysts were removed from the reactor and kept under air in screw-cap vials at room temperature. Characterization of spent catalysts was performed with XRD, TEM, and TG-DTA (air) techniques.

The results of XRD measurements with spent catalysts are shown in Fig. 6. A set of three readily distinguishable peaks at 2Θ 44.5°, 51.8°, and 76.4° of patterns can undoubtedly be assigned to a metallic nickel phase, as the peaks were typical of X-ray reflection from the (111), (200), and (220) atomic planes of nickel. A broadened symmetric peak of low intensity at 2Θ 26.6° corresponded to X-ray reflection from the (111) plane of graphite. It can be seen that such a peak was minimal in intensity for *cp*-Ni/$MgAlO_x$ spent catalyst (pattern A), suggesting that the catalyst was less loaded with graphitic coke or, alternatively, was covered with XRD nondetectable amorphous carbonaceous deposit.

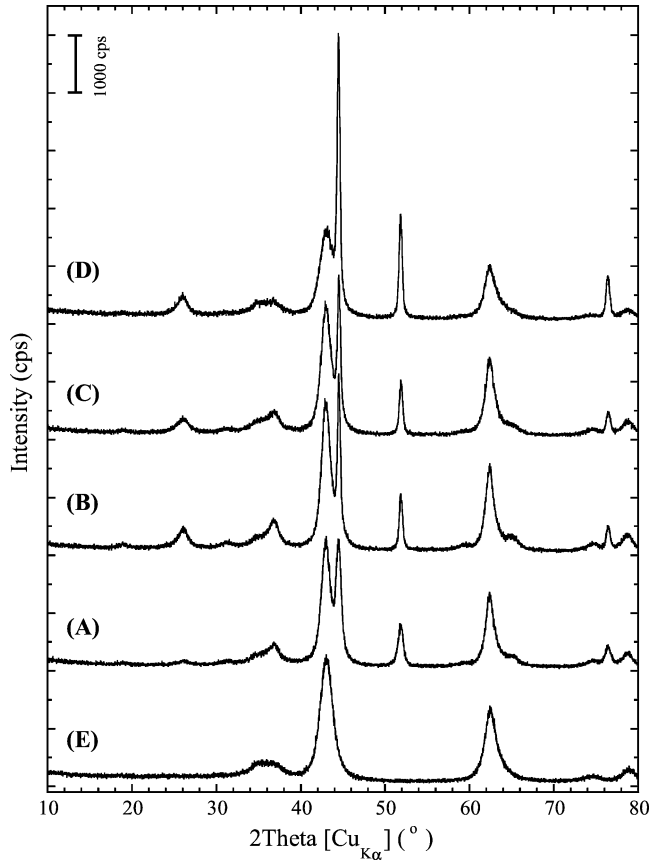

Fig. 6. X-ray powder diffraction patterns of Ni–Mg–Al mixed oxides and blank $MgAlO_x$ after being subjected to DRM at 800 °C for 6 h: *cp*-Ni/$MgAlO_x$ (A), *ae*-Ni/$MgAlO_x$ (B), *rc*-Ni/$MgAlO_x$ (C), *tr*-Ni/$MgAlO_x$ (D), and nickel-free $MgAlO_x$ (E).

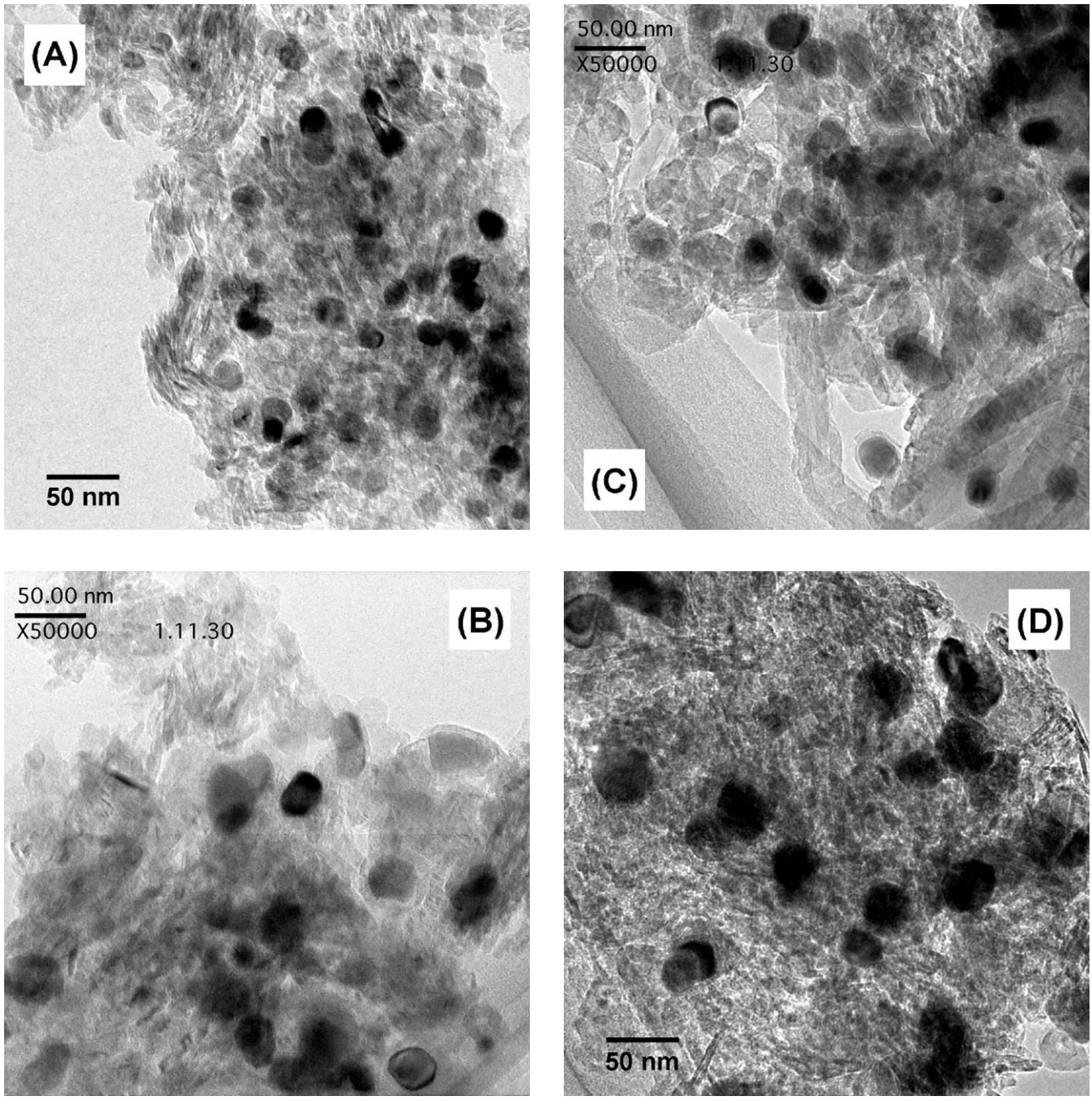

Fig. 7. TEM micrograph images of Ni–Mg–Al mixed oxide catalysts after exposure to DRM reaction at 800 °C for 6 h: *cp*-Ni/$MgAlO_x$ (A), *ae*-Ni/$MgAlO_x$ (B), *rc*-Ni/$MgAlO_x$ (C), and *tr*-Ni/$MgAlO_x$ (D).

In addition, the spent $MgAlO_x$ (blank) sample revealed XRD pattern (E) characteristic of periclase MgO, without any peaks potentially attributable to graphitic carbon.

Based on the broadening of the well-resolved peak at 2Θ 51.8° of X-ray reflection from the $Ni_{(200)}$ atomic plane, an assessment of the average size of metallic nickel crystallites was made (Table 2). The lowest value (161 Å) was retrieved for Ni-catalyst derived from *cp*-MgAl–NiY LDH. Then followed *rc*-Ni/$MgAlO_x$ with a crystallite size of 229 Å. Catalysts prepared by anion-exchange and traditional (i.e., precipitation of cations) techniques revealed nearly the same crystallite sizes (242 Å).

A similar trend was revealed with TEM observations. The smallest in size nickel particles were observed over the spent *cp*-Ni/$MgAlO_x$ catalyst (Fig. 7A). TEM micrograph images of both *ae*-Ni and *rc*-Ni/$MgAlO_x$ spent catalysts demonstrated nickel particles larger in size and less uniformly distributed (Figs. 7B and 7C). The biggest metallic nickel crystallites were observed over the spent *tr*-Ni/$MgAlO_x$ catalyst (D). This finding clearly indicated that the nickel in-

Table 2
Average size of metallic nickel crystallites for LDH-derived catalysts subjected to DRM at 800 °C for 6 h

Spent catalyst	Nickel crystallite size (Å)[a]
cp-Ni/$MgAlO_x$	161
ae-Ni/$MgAlO_x$	242
rc-Ni/$MgAlO_x$	229
tr-Ni/$MgAlO_x$	242

[a] Estimates were made using the Scherrer equation for the XRD peak at 2Θ 51.8°, assigned to the reflection from the $Ni_{(200)}$ plane.

troduced into the LDH precursor by traditional method of cation co-precipitation was less sustainable against sintering under DRM reaction conditions employed in this study. TEM data obtained also help elucidate the difference in induction times for gaining catalytic activity of nonreduced catalysts (Fig. 5). As was demonstrated with temperature-programmed reduction studies [46], the larger the particles of supported nickel oxide, the more easily they could be reduced to metallic nickel. In our studies, an induction time was observed with nonreduced *cp*-Ni/$MgAlO_x$ catalysts bearing the smallest nickel particles nearly triple that of nonreduced *tr*-Ni/$MgAlO_x$ catalyst.

It was experimentally found that the process of coke formation during DRM at 800 °C also depended on the manner in which the nickel was introduced into a particular $MgAlO_x$-supported catalyst. Thus, temperature-programmed oxidation of spent nickel catalysts, done with the TG-DTA technique, revealed the order of catalyst coking as *cp*-Ni/ < *rc*-Ni/ $\leqslant$ $MgAlO_x$ (blank) < *ae*-Ni/ < *tr*-Ni/$MgAlO_x$ (Table 3).

The detailed TG-DTA data for spent nickel catalysts and blank Mg–Al mixed oxide are presented in Fig. 8. An interesting feature of sample weight behavior can be seen from TG-profiles of spent Ni-catalysts. The initial step of reduction in their weight occurred at temperatures of 250–300 °C, which could be assigned to thermal desorption of water and CO_2 adsorbed (as samples were kept under air) and removal of easily oxidizable carbonaceous species. A viewable increase in sample weight occurred thereafter to 410–450 °C, which we ascribe to oxidation of surface-supported metallic nickel to a nickel oxide phase. The largest reduction in sample weight proceeded at 480 to 640 °C; it was related to oxidation of coke to CO and CO_2 (CO_x). As oxidation of carbonaceous deposit with oxygen in air is an exothermic process, DTA under an oxidative atmosphere can be applied to monitoring the decoking of catalyst. As can be seen in Fig. 8A*, no considerable exothermic peaks were observed in a temperature range of 400 to 700 °C, indicating that a minor amount of coke was deposited onto *cp*-Ni/$MgAlO_x$ catalyst surface. DTA profiles of spent *ae*- and *rc*-Ni/$MgAlO_x$ catalysts (Figs. 8B* and 8C*) revealed two easily distinguishable exothermic peaks located near 470 and 600 °C, which implied that at least two kinds of carbonaceous deposits different in resistance to oxidation were formed. The main part of coke deposited onto *tr*-Ni/$MgAlO_x$ catalyst was oxidatively removed at 480–540 °C (profile D* in Fig. 8). The rest required a higher temperature (600–640 °C) for oxidative removal. Oxidation of coke deposited over nickel-free $MgAlO_x$ support occurred at a temperature notably higher than those of spent Ni-containing catalysts. As can be seen in Fig. 8E*, a strong exothermic peak assigned to coke oxidation appeared at 525 °C. These results clearly indicated the promoting role of oxidized nickel in removing catalytically deposited coke (C_{dep}). In our opinion, the supported nickel oxide could facilitate the dissociative adsorption of molecular oxygen to give a reactive oxygen species (O^*) responsible for coke oxidation,

$$O_2 = 2O^*, \tag{5}$$

$$xO^* + C_{dep} = CO_x\uparrow. \tag{6}$$

Table 3
Coke deposition onto surface of nickel catalysts synthesized via LDH precursors

Spent catalyst	Amount of coke (wt%)[a]
cp-Ni/$MgAlO_x$	5.3
ae-Ni/$MgAlO_x$	15.8
rc-Ni/$MgAlO_x$	13.1
tr-Ni/$MgAlO_x$	19.2
$MgAlO_x$ (blank)	13.5

Nonreduced catalysts were subjected to DRM at 800 °C for 6 h.
[a] Coke deposition was quantified by thermogravimetry.

3.4. Magnesium–aluminum mixed oxide as support for nickel catalysts: evaluation of thermal stability

Preliminary calcination of a catalyst or catalyst precursor at a temperature higher than that of catalytic tests is a common experimental procedure in catalyst preparation. Such a treatment strengthens the interaction of a target catalyst component(s) with an oxide support, resulting in the formation of more stable catalyst [47]. For nickel catalysts supported on magnesia, such a treatment, however, leads to the formation of $Ni_xMg_{(1-x)}O$ solid solutions. As a result, a considerable amount of nickel diffuses from the catalyst surface into the bulk of the support, where it becomes irreducible and therefore ineffective for catalysis [46,48].

To prepare Ni–Mg–Al mixed oxides with a high specific surface area and avoid formation of solid solutions, we calcined Ni-containing LDHs at 500 °C. Nevertheless, catalytic properties of the resultant mixed oxides toward DRM reaction were tested at 800 °C. This might raise a reasonable question as to the stability of Mg–Al mixed oxide support during the DRM test reaction done at a temperature 300 °C higher. Together with nickel sintering, one might expect the formation of an Mg–Al spinel-like phase, which is known to readily form at temperatures higher than 500 °C.

The first reference sample selected for comparison was a physical mixture of fine powders of MgO and α-alumina

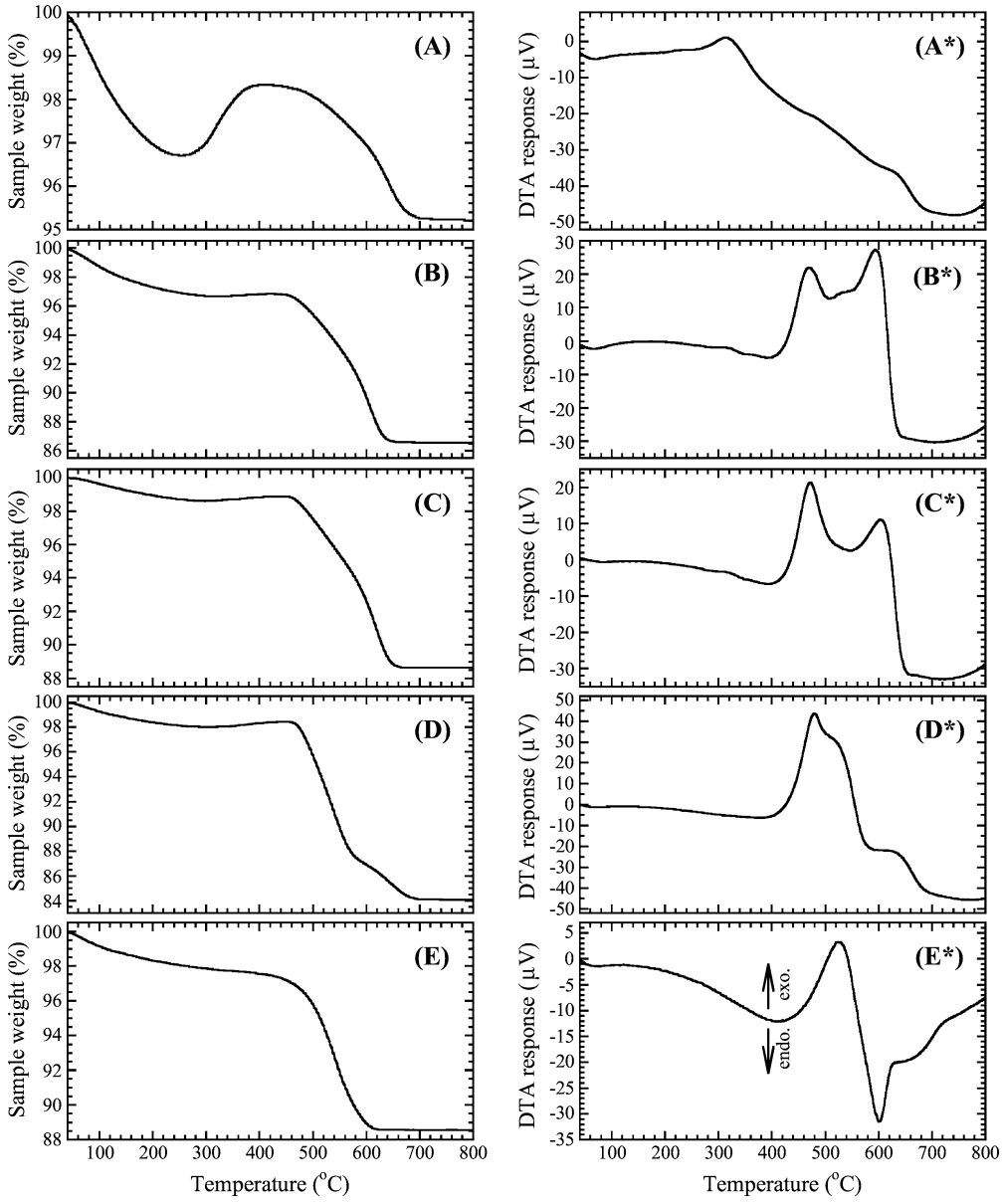

Fig. 8. TG-DTA behavior of spent catalysts under air: *cp*-Ni/MgAlO$_x$ (A, A*), *ae*-Ni/MgAlO$_x$ (B, B*), *rc*-Ni/MgAlO$_x$ (C, C*), *tr*-Ni/MgAlO$_x$ (D, D*), and MgAlO$_x$ (E, E*).

taken with a 1 : 1 molar ratio favorable for $MgAl_2O_4$ spinel formation. Such a mixture was calcined in air at 500 °C for 16 h and at 800 °C for 6 h, followed by XRD detection of phases formed upon calcination. Both calcined samples revealed XRD patterns identical to that of a noncalcined magnesia–alumina physical mixture recorded at room temperature, which was in full agreement with literature reporting that a much higher temperature must be applied in order to initiate solid-state reactions in the physical mixture [49].

Another reference material included the solid obtained by water evaporation from an aqueous solution of Mg(II) and Al(III) nitrates taken with 1 : 2 mole ratio. Portions of the solid were calcined at 500, 800, and 1000 °C. The resulting XRD patterns are shown in Fig. 9 as "spectra" A, B, and C. It is seen that the formation of the $MgAl_2O_4$ spinel phase started at 500 °C, as characteristic reflection peaks at 2Θ 36.8°, 44.8°, and 65.2° appeared. An increase in calcination temperature to 1000 °C resulted in a formation of true spinel phase demonstrating a set of sharp and intensive X-ray reflection peaks. On the contrary, when MgAl–CO_3 hydrotalcite was calcined in air at 500 °C for 16 h, the resultant Mg–Al mixed oxide revealed XRD pattern (D) similar to that of periclase MgO. However, when such mixed oxide was further calcined at a higher temperature (i.e., 1000 °C), the XRD-detectable spinel phase was formed (pattern E). The last pattern (F) shown in the figure is of MgAlO$_x$ mixed oxide derived from MgAl–CO_3 synthetic hydrotalcite and further exposed to the DRM reaction at 800 °C for 6 h. As can be seen from the comparison of patterns F and D, the spent MgAlO$_x$ blank

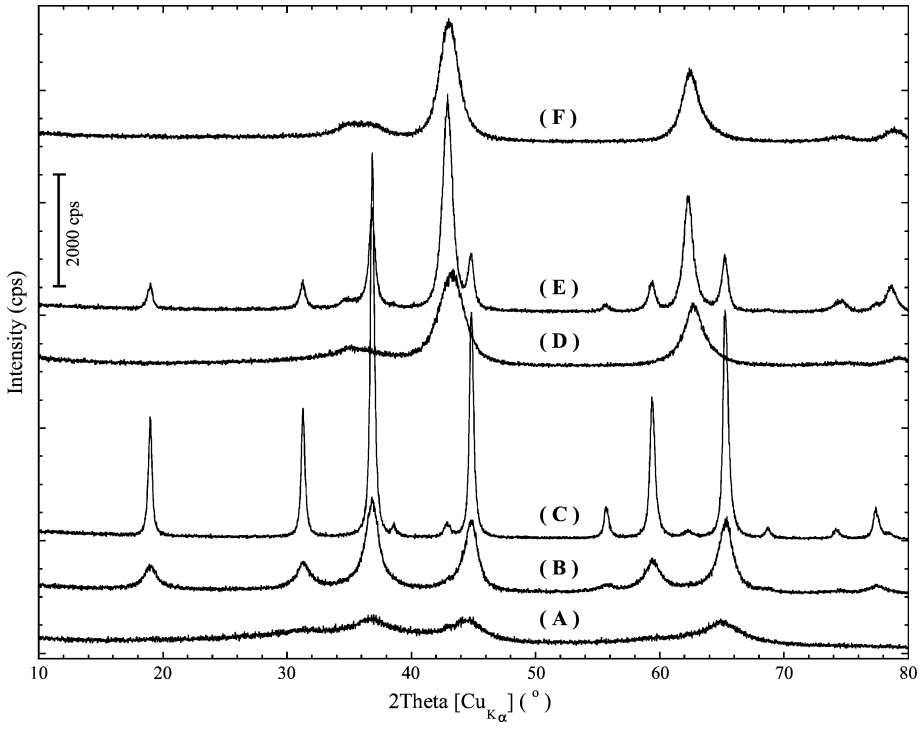

Fig. 9. Powder XRD patterns of Mg–Al mixed oxides derived from various solid precursors: Mg(II) and Al(III) nitrates calcined at 500 °C for 16 h (A), at 800 °C for 6 h (B), and at 1000 °C for 6 h (C), MgAl–CO_3 calcined at 500 °C for 16 h (D), sample (D) additionally calcined at 1000 °C for 6 h (E), and sample (D) exposed to DRM at 800 °C for 6 h (F).

sample maintained the phase composition of periclase MgO. These results indicated that Mg–Al mixed oxide prepared from hydrotalcite by calcination in air at 500 °C appeared to be a stable support material suitable for employment in the DRM reaction at a temperature higher than that of preliminary calcination. It should be here pointed out that such a material was also stable in the presence of supported nickel. As was shown above (Fig. 6), XRD analysis of spent nickel catalysts revealed the presence of metallic nickel, graphite (as of carbonaceous deposit), and periclase MgO phases with no XRD-detectable impurities of $MgAl_2O_4$ or $NiAl_2O_4$ spinels.

4. Conclusion

A new strategy of preparing active and selective Ni–Mg–Al mixed oxide catalysts derived from layered double hydroxide precursors was reported. Alternatively to the traditional technique of cations co-precipitation, the nickel was introduced via precomplexation with $EDTA^{4-}$ ligand and incorporation of the resultant anionic nickel chelate into LDH structure by co-precipitation, anion exchange, and reconstruction reactions. The corresponding Ni–Mg–Al mixed oxides demonstrated high and sustainable catalytic activity and selectivity in dry reforming of methane at 800 °C. Such catalysts did not require preliminary reductive activation treatment but needed 0.5 to 1.5 h induction time to approach maximal activity. It was also shown that such LDH-derived catalysts offered CH_4 and CO_2 conversions markedly higher than those attained with catalysts prepared by sol–gel and cellulose-template methods.

The reported synthetic approach is sufficiently general to allow incorporating various transition metals (other than nickel) into LDH materials and preparing catalysts supported on Mg–Al mixed oxide.

Acknowledgments

This work was supported by the Japan Society for the Promotion of Science (JSPS) and the New Energy and Industrial Technology Development Organization (NEDO). The authors sincerely thank Dr. Albert N. Shigapov (Krasnoyarsk State Academy of Non-Ferrous Metals and Gold, Krasnoyarsk, Russian Federation) for the donation of *ctm*-nickel catalyst.

References

[1] M.C.J. Bradford, M.A. Vannice, Catal. Rev. Sci. Eng. 41 (1999) 1.
[2] M.C.J. Bradford, M.A. Vannice, Appl. Catal. A 142 (1996) 73.
[3] S.C. Tsang, J.B. Claridge, M.L.H. Green, Catal. Today 23 (1995) 3.
[4] J.N. Armor, Appl. Catal. A 176 (1999) 159.
[5] D. Dissanayake, M.P. Rosynek, K.C.C. Kharas, J.H. Lunsford, J. Catal. 132 (1991) 117.
[6] A.T. Ashcroft, A.K. Cheetham, M.L.H. Green, P.D.F. Vernon, Nature 352 (1991) 225.
[7] M.A. Pena, J.P. Gomez, J.L.G. Fierro, Appl. Catal. A 144 (1996) 7.

[8] D.L. Trimm, Catal. Rev. Sci. Eng. 16 (1977) 155.
[9] D.L. Trimm, Catal. Today 49 (1999) 3.
[10] J.B. Claridge, M.L.H. Green, S.C. Tsang, A.P.E. York, A.T. Ashcroft, P.D. Battle, Catal. Lett. 22 (1993) 299.
[11] J.-H. Kim, D.J. Suh, T.-J. Park, K.-L. Kim, Appl. Catal. A 197 (2000) 191.
[12] T. Horiuchi, K. Sakuma, T. Fukui, Y. Kubo, T. Osaki, T. Mori, Appl. Catal. A 144 (1996) 111.
[13] F. Cavani, F. Trifiro, A. Vaccari, Catal. Today 11 (1991) 173.
[14] A. Vaccari, Catal. Today 41 (1998) 53.
[15] S.P. Newman, W. Jones, New J. Chem. 22 (1998) 105.
[16] B.F. Sels, D.E. De Vos, P.A. Jacobs, Catal. Rev. Sci. Eng. 43 (2001) 443.
[17] F. Basile, L. Basini, M. D'Amore, G. Fornasari, A. Guarinoni, D. Matteuzzi, G. Del Piero, F. Trifiro, A. Vaccari, J. Catal. 173 (1998) 247.
[18] T. Shishido, M. Sukenobu, H. Morioka, M. Kondo, Y. Wang, K. Takaki, K. Takehira, Appl. Catal. A 223 (2002) 35.
[19] K. Schulze, W. Makowski, R. Chyzy, R. Dziembaj, G. Geismar, Appl. Clay Sci. 18 (2001) 59.
[20] K. Schulze, PhD thesis, Gerhard–Mercator University, Duisburg, Germany, 2001.
[21] T. Shishido, M. Sukenobu, H. Morioka, R. Furukawa, H. Shirahase, K. Takehira, Catal. Lett. 73 (2001) 21.
[22] A.I. Tsyganok, K. Suzuki, S. Hamakawa, K. Takehira, T. Hayakawa, Chem. Lett. 24 (2001).
[23] A.I. Tsyganok, K. Suzuki, S. Hamakawa, K. Takehira, T. Hayakawa, Catal. Lett. 77 (2001) 75.
[24] B.F. Sels, D.E. De Vos, P.A. Jacobs, Tetrahedron Lett. 37 (1996) 8557.
[25] B. Sels, D. De Vos, M. Buntinx, F. Pierard, A. Kirsch-De Mesmaeker, P. Jacobs, Nature 400 (1999) 855.
[26] K. Bahranowski, G. Bueno, V.C. Corberan, F. Kooli, E.M. Serwicka, R.X. Valenzuela, K. Wcislo, Appl. Catal. A 185 (1999) 65.
[27] T. Hibino, A. Tsunashima, Chem. Mater. 10 (1998) 4055.
[28] J. Rocha, M. del Arco, V. Rives, M.A. Ulibarri, J. Mater. Chem. 9 (1999) 2499.
[29] F. Millange, R.I. Walton, D. O'Hare, J. Mater. Chem. 10 (2000) 1713.
[30] The Merck Index: An Encyclopedia of Chemicals, Drugs, and Biologicals, 12th ed., Merck & Co., Whitehouse Station, 1996, p. 1470.
[31] S. Suzuki, T. Hayakawa, S. Hamakawa, K. Suzuki, T. Shishido, K. Takehira, Stud. Surf. Sci. Catal. 119 (1998) 783.
[32] T. Hayakawa, S. Suzuki, J. Nakamura, T. Uchijima, S. Hamakawa, K. Suzuki, T. Shishido, K. Takehira, Appl. Catal. A 183 (1999) 273.
[33] A.N. Shigapov, H.-W. Jen, G.W. Graham, W. Chun, R.W. McCabe, Stud. Surf. Sci. Catal. 130 (2000) 1373.
[34] A.N. Shigapov, G.W. Graham, R.W. McCabe, H.K. Plummer Jr., Appl. Catal. A 210 (2001) 287.
[35] A.M. Gadalla, B. Bower, Chem. Eng. Sci. 43 (1988) 3049.
[36] A.M. Gadalla, M.E. Sommer, J. Am. Ceram. Soc. 72 (1989) 683.
[37] E. Ruckenstein, Y.H. Hu, Appl. Catal. A 133 (1995) 149.
[38] Y.H. Hu, E. Ruckenstein, Catal. Lett. 36 (1996) 145.
[39] E. Ruckenstein, Y.H. Hu, Appl. Catal. A 154 (1997) 185.
[40] Y.H. Hu, E. Ruckenstein, Catal. Lett. 43 (1997) 71.
[41] E. Ruckenstein, Y.H. Hu, Chem. Innov. 30 (2000) 39.
[42] K. Tomishige, K. Fujimoto, Catal. Surv. Japan 2 (1998) 3.
[43] K. Tomishige, O. Yamazaki, Y. Chen, K. Yokoyama, X. Li, K. Fujimoto, Catal. Today 45 (1998) 35.
[44] K. Tomishige, Y. Chen, K. Fujimoto, J. Catal. 181 (1999) 91.
[45] Y.-G. Chen, K. Tomishige, K. Yokoyama, K. Fujimoto, J. Catal. 184 (1999) 479.
[46] A. Parmaliana, F. Arena, F. Frusteri, N. Giordano, J. Chem. Soc. Faraday Trans. 86 (1990) 2663.
[47] G.A. Somorjai, Introduction to Surface Chemistry and Catalysis, Wiley–Interscience, New York, 1994.
[48] F. Arena, F. Frusteri, A. Parmaliana, L. Plyasova, A.N. Shmakov, J. Chem. Soc. Faraday Trans. 92 (1996) 469.
[49] L. Schreyeck, A. Wlosik, H. Fuzellier, J. Mater. Chem. 11 (2001) 483.